The Origin, Development, and Conformation of Amorphous Inclusion Body Components in Tobacco Etch Virus-Infected Cells

John H. Andrews and T. A. Shalla

Department of Plant Pathology, University of California, Davis 95616.
The senior author's present address is the A.R.C. Unit of Developmental Botany, University of Cambridge, Cambridge, CB3 ODY England.
Accepted for publication 30 April 1974.

ABSTRACT

The origin, development, and conformation of pinwheel inclusion bodies induced by tobacco etch virus (TEV) were studied in tobacco (*Nicotiana tabacum* L. 'Havana 425') root tips. Pinwheels were abutted to cell walls at plasmodesmata in cells examined during the early stages of infection. With time, there was an increasing tendency for pinwheels to be located free in the cytoplasm and to have more and longer arms, fused arms, and opened central cores. Pinwheel arms appeared triangular when examined in serial sections. On the basis of results obtained by freeze-etching and the use of different fixatives, it was concluded that pinwheels are real entities, not artifacts of sample preparation. Evidence is presented to show that they originate at plasmodesmata and may be released into the cytoplasm at a later stage of development, and that the inclusion as a whole is conically shaped, at least during the early stages of formation.

Phytopathology 64:1234-1243

In host cells, certain rod-shaped plant viruses induce the formation of amorphous inclusion bodies which are characterized ultrastructurally by the presence of numerous components, each consisting of curved arms radiating outward from a central core. These components, which have been called cylindrical inclusions, appear in cross- and longitudinal sections as pinwheels and bundles, respectively (8). Most viruses with which these characteristic structures are associated belong to the potato virus Y (PVY) group (5), of which tobacco etch virus (TEV) is a member. For the sake of convenience and clarity, the terms "amphorous inclusion body components", "cylindrical inclusions", and "bundles" will be referred to simply as "pinwheels" or "inclusions" throughout this text.

Pinwheels were first reported by Cremer et al. (7) in cells infected by narcissus yellow stripe virus. Somewhat later Rubio-Huertos and Garcia-Hidalgo (26), and Matsui and Yamaguchi (21, 22) noted their occurrence in TEV-infected cells. At this time they had not been named as such, and no one had made a clear distinction between aggregates of virions and the pinwheels themselves. In fact, what Matsui and Yamaguchi (21) described as being three kinds of viral masses, Edwardson (8, 9) interpreted correctly as different aspects of a single type of inclusion.

On the basis of evidence obtained from serial sections, Cremer et al. (7) stated that pinwheels (referred to by them as "oblong bodies") were membranous, mat-shaped structures with irregular, gradually changing contours. Rubio-Huertos and Lopez-Abella (27) reconstructed what is essentially a cylindrical structure from serial sections of pinwheels in infected pepper plants. However, elucidation of the ultrastructure and conformation of pinwheels is generally credited to the classic series of papers by Edwardson and his colleagues (e.g. 8, 9, 11). Inclusions induced by TEV were interpreted by being cylindrical, despite the presence in negatively stained preparations of triangular plates which were considered to be laminated aggretates. These views have since been extended by studies of pinwheels induced by various other viruses, mostly of the PVY group (see, for example 10, 12, 32). A problem with using the terms pinwheel and cylindrical inclusion interchangeably is that, by implication, all pinwheels are assumed to be cylindrical, and this dogma has become entrenched in the literature (e.g. 24). In the absence of definitive evidence in each instance, such as that obtained by serial sectioning, this assumption is not valid.

The origin of pinwheels is not well understood. It is important in this context to differentiate clearly between association and origin. Association of pinwheels with cellular membrane systems, including the plasmalemma and endoplasmic reticulum (ER) has been well established (e.g. 2, 4, 14, 20, 24). Fewer reports have dealt with the origin of these inclusions. After examining cells infected with wheat spindle streak mosaic virus (WSSMV), Hooper and Wiese (15) initially reported that aggregates of plates fragmented to produce pinwheels. However, this theory was discarded later in favor of another which envisaged pinwheels being formed on the surfaces of double membranes (16). Plasmodesmata were considered to be the site of origin of pinwheels induced by sweet potato russet crack virus (19, 20).

A major unanswered question regarding pinwheels is their role in infected cells. Knowledge of the origin, development, and conformation of these inclusions is basic to an eventual understanding of their function. To obtain this information, an approach different from those noted above was used. Our study involved the sequential development of pinwheels in root tips of tobacco plants systemically infected with TEV. Our results support the idea that pinwheels originate at plasmodesmata. In addition, we present evidence that, while still attached to the plasmalemma, they grow in a conical, rather than a cylindrical manner. The significance of this site of origin and such a developmental pattern to the normal ultrastructure and physiology of host cells is discussed. Data from freeze-etched samples and the use of different fixatives support a conclusion that the pinwheels are real structures, although entities whose biological role still remains unknown.

MATERIALS AND METHODS.—A severe strain of TEV, in dried leaves of tobacco plants (*Nicotiana tabacum* L. 'Havana 425'), was obtained from Dr. R. J. Shepherd (stock culture #159, Wisconsin isolate), and maintained thereafter by passage through tobacco plants growing in a greenhouse.

For most experiments, plants were grown in a controlled environment chamber under the following regime: days 27 C, nights 18 C; 14-h photoperiod; approximately 21,000 lux at pot level.

Tobacco seedlings were transplanted about 1 mo after sowing to 12.5-cm diam plastic pots containing U.C. soil mix (3). Plants were inoculated mechanically at the three- to four-leaf stage. Plants used for freeze-etching studies were grown in a greenhouse. Noninoculated plants were grown under the same conditions for controls.

Preparation of tissue sections for electron microscopy.—Following preliminary experiments to determine the rate of movement of virus into the roots, plants were harvested 17-21 days after inoculation. Root tips (as used here "root tip" refers to the distal 8 mm of the root and thus includes the root cap, apical meristem, elongation, and root hair regions) were removed, washed in distilled water, subdivided, and the portions categorized as belonging to one of the following three arbitrarily-defined regions: (i) root hair zone–that region where root hairs were visible macroscopically or with ×20 magnification; (ii) elongation zone–the region between the root hair zone and a point ca. 1,200 μm from the root apex; and (iii) apical meristem–the apical 1,200μm, exclusive of the root cap. Individual root tips and the subdivided portions were kept separate, thus allowing a developmental sequence of pinwheels to be followed.

Generally, root pieces were fixed at room temp in 3% glutaraldehyde in 0.05 M phosphate buffer, pH 6.8 (1.5 h), postfixed in phosphate-buffered 2% osmium tetroxide (2 h), dehydrated with acetone, and embedded in low-viscosity epoxy resin (31). Sections, 50- to 60-nm thick, were cut with a diamond knife on a Porter Blum microtome and mounted on 48-μm (300-mesh) copper grids. Serial sections were mounted on bar grids (E. F. Fullam, Inc.) by the collodion-coated disk method of Williams and Kallman (33). Uranyl acetate and lead citrate were used as stains.

To ascertain the effect of fixatives on pinwheel

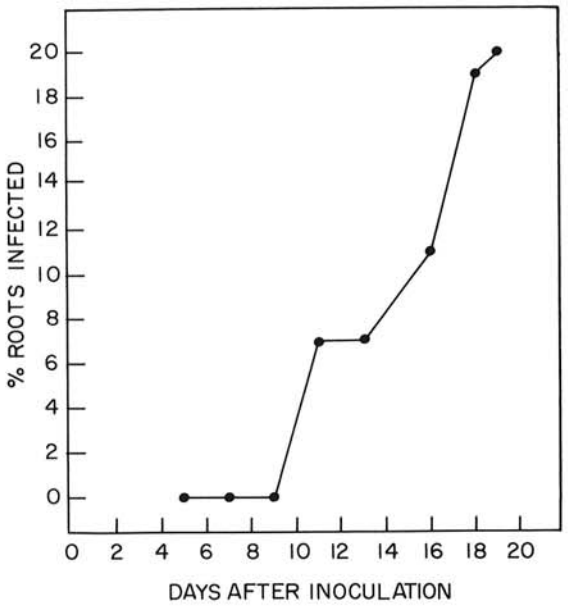

Fig. 1. Percent infection by tobacco etch virus of tobacco roots with time after mechanical inoculation of leaves of young plants (three- to four-leaf stage) growing in a controlled environment chamber. At each sampling time ca. 60 roots from 12-20 plants were assayed by the dip method.

appearance, some roots were divided longitudinally; one-half was prepared by the method noted above and the other with either of the following fixatives: (i) 3% glutaraldehyde in 0.05 M phosphate buffer (pH 6.8) with 0.2% mercaptoethanol, followed by buffer rinses containing 0.2% mercaptoethanol; (ii) 1% osmium tetroxide in phosphate buffer containing 0.25 M sucrose (25).

Thin-sections of cortical cells in the three regions of the root were correlated with free-hand thick sections (ca. 5-μm) through the stele. This permitted an approximation of the extent of cellular differentiation which aided in comparing thin-sections from different infected roots.

Instrumentation.—For transmission electron microscopy, specimens were examined either with an RCA EMU 3H at 50 kV or a Hitachi HU-11 at 75 kV. A carbon grating replica was used to determine instrument magnifications.

Preparation of tissue for light microscopy.—To correlate ultrastructural observations and infectivity assays with the gross anatomy of root tips, roots were excised, fixed in Craf III, dehydrated in an ethyl alcohol-TBA series and embedded in Tissuemat (m.p. 52-54 C, Fisher Scientific Co.) using standard procedures (28). Longitudinal sections, 10-μm thick, were cut on a rotary microtome, affixed to microscope slides and stained with safranin-fast green.

Preparation of tissue for freeze-etching.—Elongation and meristem regions from infected or healthy roots were cut into small pieces (ca. 0.2 - 0.5 mm) and infiltrated for 1.5 - 2.5 h with a graded series of glycerol solutions up to 25%. Droplets containing the tissue were mounted on 3-mm copper disks, frozen in liquid freon, and stored in liquid nitrogen until used. Freeze-etching was done with a Balzers Model BA 360. Specimens were fractured with platinum-alloy razor blades, then subjected to a standard etch time of 20 s at −100 C. They were replicated by platinum-carbon shadowing, followed by carbon reinforcement. Replicas were cleaned by flotation on commercial bleach (10%, 30%, 100%) for 15 h, followed by sulfuric acid (10%, 30%, 70%) for 11 h. Cleaned replicas were retrieved from distilled water on uncoated 300-mesh grids.

For comparison, leaf cells from healthy or infected plants were obtained by an enzymatic digestion method (1), and processed as above prior to freeze-etching.

Assay methods.—Roots were routinely verified as being infected by the presence of triangular plates and virus particles in negatively stained (1% potassium phosphotungstate or 2% ammonium molybdate), or shadowed, preparations (11) from a 5-10 mm sample basal to the regions used for ultrastructural studies. The validity of this method was substantiated by examination of thin-sections or by assay of roots on leaves of shaded *Chenopodium amaranticolor* Coste & Reyn., a local lesion host for TEV.

To ascertain the relative amount of virus in the meristematic, elongation, and root hair regions, respectively, a 0.8-mm sample was taken from each zone, combined with similar samples from five other roots, ground in 0.1 ml phosphate buffer (pH 7.0) and assayed on leaves of *C. amaranticolor*.

RESULTS.—*Pinwheel development.*—Preliminary studies were made to devise a reliable and convenient assay system for detecting infected roots, since these could not be distinguished by symptoms. Root samples which were rated positive, based on the presence of triangular plates and virus particles in dip preparations (11), also produced local lesions on *C. amaranticolor* and displayed pinwheels in thin-sections. The correlation between these three methods was very good, with less than 5% error. Subsequently, the dip method was chosen routinely to identify infected roots because it was the most rapid.

The dip method was used to determine the rate and extent to which TEV moved into root tips (Fig. 1). Infected roots could not be detected prior to 10 days postinoculation. Between 10 and 18 days, the percentage of infected roots rose; however, by 21 days, the plants were in a deteriorating condition due to the advanced stage of infection. The interval between 17-21 days was chosen as a compromise between a good probability of any given root being infected and the desirability of utilizing plants in reasonably good condition in which the

→

Fig. 2-(a to f). Longitudinal section of a tobacco etch virus-infected tobacco root tip illustrating the regions in which pinwheels were examined, and the relative virus concn determined. **a, b, and c)** Thick-sections through the stele in the regions of the arrows representing root hair, elongation, and apical meristem zones, respectively. ×417. **d, e, and f)** Thin-sections of infected cortical cells in corresponding zones at the same level. pl, plasmalemma. ×67,750. Infectivity assay represents the total number of local lesions on five leaves of *Chenopodium amaranticolor* per root sample. Scale bars: (a, b, and c) 10 μm; (d, e, and f) 0.1 μm.

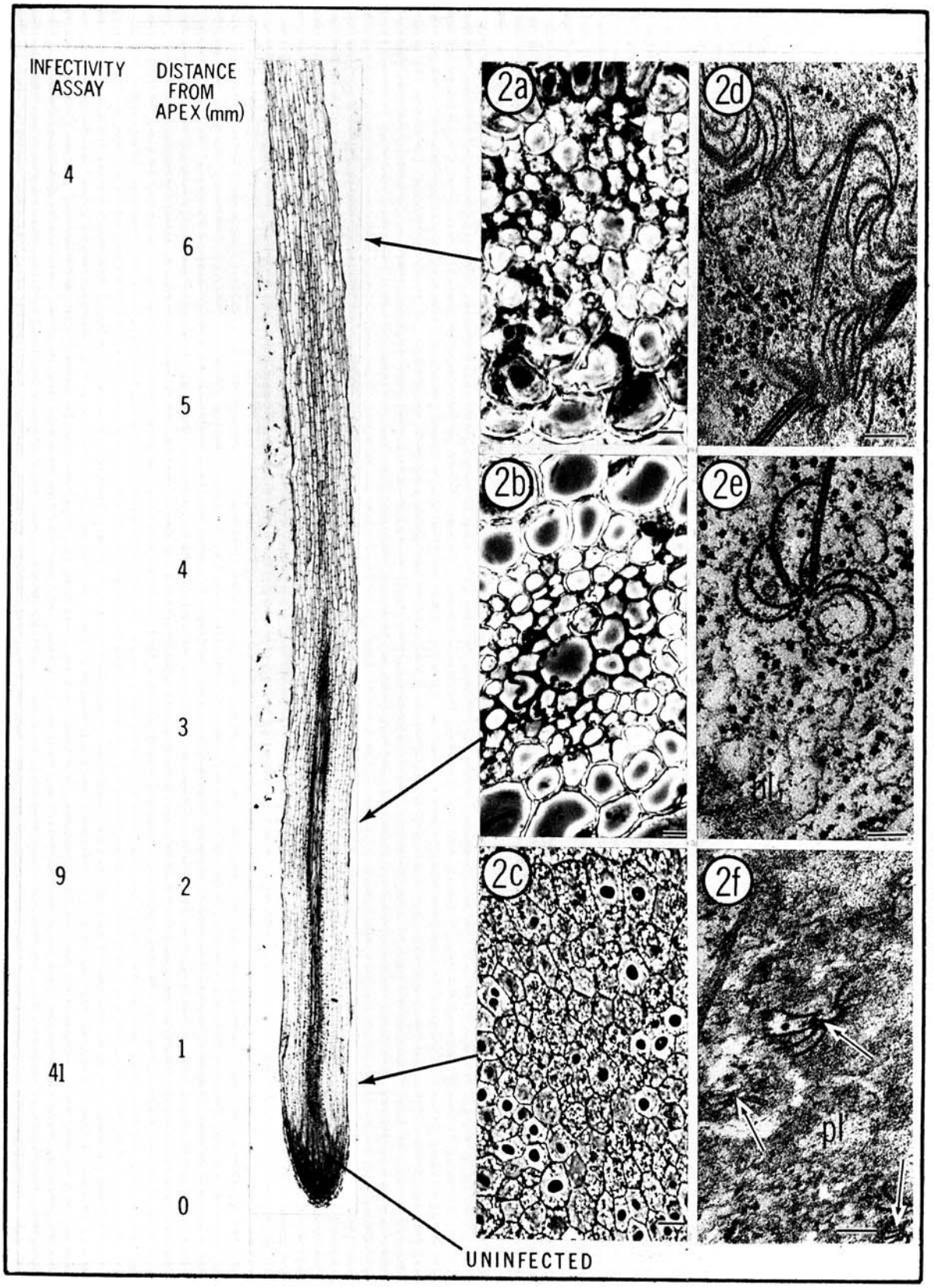
INFECTIVITY ASSAY
DISTANCE FROM APEX (mm)
4
6
5
4
3
9
2
1
41
0
2a
2d
2b
2e
pl
2c
2f
pl
UNINFECTED

sequence of pinwheel development could be followed.

Pinwheels representing those found in cortical cells of the root hair, elongation and meristem regions, are shown in Fig. 2-d, 2-e, and 2-f, respectively. Thick, free-hand sections through the stele illustrate the extent of vascular differentiation (Fig. 2-a, 2-b, and 2-c) and provide a more reliable estimate of cellular maturation than distance from the apex. Note that pinwheels in the meristem (Fig. 2-f) were small and associated with the cell wall and plasmalemma. Those present in the elongation zone (Fig. 2-e) were larger, though still generally apposed to the cell wall or close to it. Inclusions in the root hair zone (Fig. 2-d) were large, contained several fused arms, and were characteristically free in the cytoplasm. Pinwheels in the apical meristem and elongation regions were characteristically abutted to the cell wall at plasmodesmata (Fig. 3-a). Virus particles were numerous in most of the apical meristem, and were often present in massive arrays (Fig. 3-b). Whereas the apical meristem region as a whole contained significantly more virus than the other regions, based on infectivity assay and electron microscopy, a small core of cells located approximately 100-200 μm back from the apex appeared free of virus when thin-sections taken at 20-μm increments in this zone were examined with the electron microscope. Pinwheels were also commonly present in the root cap.

Data were obtained to support a developmental sequence of pinwheels (Fig. 4). The parameters considered in establishing a pattern of pinwheel ontogeny were: (i) total arm length; (ii) arm number; (iii) presence or absence of fused arms; (iv) number of arms fused; and (v) presence or absence of an intact central core. These results are based on an examination of cross sections of 75 pinwheels selected at random in thin-sections from each of the root hair, elongation and apical meristem regions.

Inclusions present in the apical meristem were characterized by shorter and slightly fewer arms (Fig 4-a and 4-b) than those further back from the root apex. Over half of the pinwheels in the apical meristem region had no fused arms (Fig. 4-d). Where present, fused arms accounted for only 20% of the total arm complement of a given inclusion (Fig. 4-c). On the other hand, most pinwheels in the elongation and root hair regions did contain fused arms (Fig. 4-d). Here they accounted for ca. 30% of the total arm number (Fig. 4-c). In all three regions of the root tip, there were about twice as many pinwheels with closed cores as those with the central cylinder open (Fig. 4-e); however, the ratio of closed to open cores was somewhat higher in the meristem than in either the elongation or root hair zones. Differences in arm length (Fig. 4-a) and fusion of arms (Figs. 4-c and 4-d) were highly significant ($P = 0.01$). Thus the evidence is in favor of real differences in arm characteristics of pinwheels from the three root regions.

To summarize, pinwheel ontogeny in root tips is characterized by the addition and growth of arms, fusion of arms, and the opening of central cores.

The pinwheel as a valid entity.—Anomalous structures, showing only a vague resemblance to pinwheels, were encountered occasionally in infected cells of some roots and consistently in other roots, almost to the exclusion of pinwheels. These bodies, herein designated as massive laminations, consisted of long arms generally fused in groups of 4-8, radiating outward from a central region.

In view of the suggestion by Hooper and Wiese (15) that pinwheels arise from aggregates of plates, and the

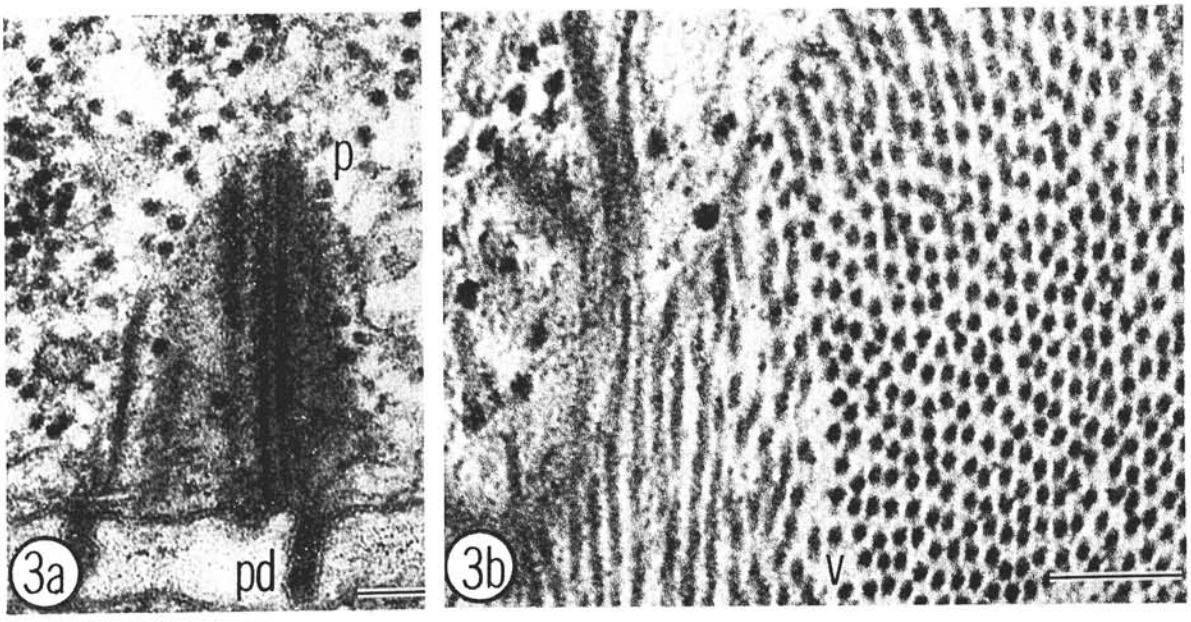

Fig. 3-(a, b) Thin-sections through the apical meristem of tobacco etch virus-infected tobacco roots. **a)** Longitudinal view of a pinwheel abutted to the cell wall at a plasmodesma. ×99,000. **b)** Array of virus particles in cross and oblique sections. ×167,000. p, pinwheel; pd, plasmodesma; v, virus. Scale bars: 0.1 μm.

ossible influence of fixatives on inclusion morphology (18), it was considered important to determine whether the classical pinwheel shape was legitimate. To establish what, if any, relationship existed between pinwheels and massive laminations, different chemical fixatives and freeze-etching techniques were used.

The presence of pinwheels did not appear to be affected by fixation under the following conditions: glutaraldehyde in the presence of a reducing agent as the sole fixative, or osmium in phosphate buffer containing sucrose. Massive laminations appeared with all fixation conditions.

Typical pinwheels were also observed in infected cells prepared by freeze-etching (Fig. 5-b). Triangular structures, presumably individual pinwheel arms and virus particles were seen in some preparations. The micrograph presented in Fig. 5-a is of a control from a noninfected root tip.

Glycerol, used as a cryoprotectant in the freeze-etch studies, is known to be phytotoxic at high concns over a prolonged time (23). As a compromise, tissues were infiltrated gradually up to 25% glycerol, thereby achieving a balance between reduced ice crystal formation and minimum damage to host cells. When

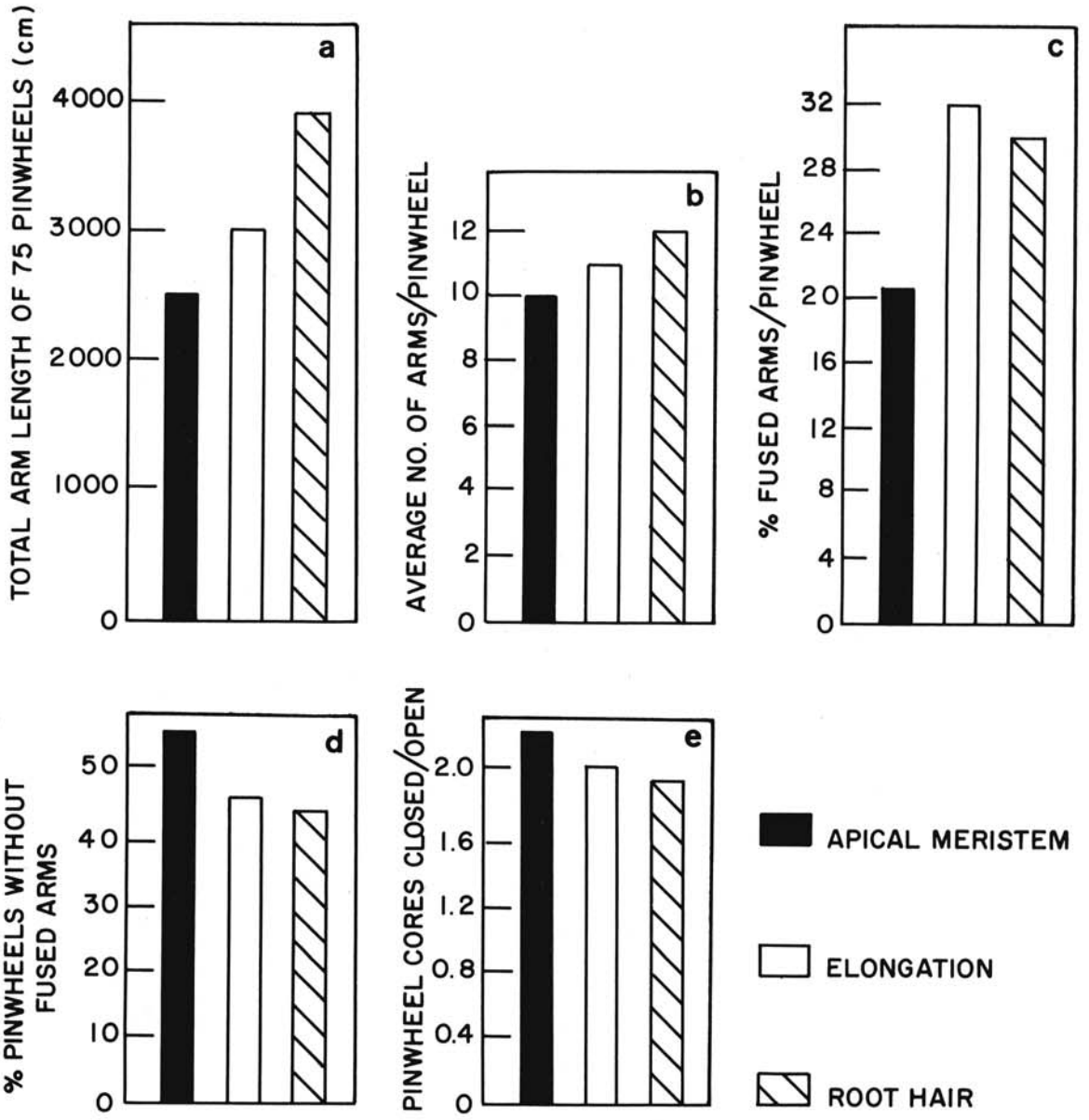

Fig. 4-(a to e). Characteristics of pinwheels present in the apical meristem, elongation, and root hair regions of tobacco etch virus-infected tobacco root tips. Data based on observations of 75 inclusions selected at random from each zone. Analysis of variance showed **a)** highly significant differences for arm length, **b)** number of arms per pinwheel, **c)** % fused arms, **d)** percentage of pinwheels without fused arms, as a function of root region, and **e)** ratio of closed to open pinwheel cores.

samples were infiltrated with glycerol, then processed for thin-sectioning, there were no serious changes in cellular ultrastructure or in the appearance of the pinwheels. These observations are consistent with those of Fineran (13) who also examined glycerol-infiltrated root tips.

Thus, typical pinwheels are found under various conditions of chemical fixation and in freeze-etch samples. From this it is concluded that they are real structures in infected cells and are not an artifact arising during preparation of tissue for electron microscopy. Additional experiments demonstrated that with time the number of massive laminations increased at the expense of pinwheels. This suggests that in the late stage of infection, pinwheels fragment to produce these large, anomalous structures.

Origin of pinwheels.—Virtually all of the pinwheels observed in longitudinal view in the apical meristem, and most of those in the elongation region, were abutted to the cell wall as shown in Fig. 3-a. When similar inclusions were viewed in cross section, they could be traced to plasmodesmata if serial sections were analyzed (Table 1). Of 35 pinwheels, 29 (83%) could be traced to plasmodesmata. The remainder were always apposed to the wall in regions of plasmodesmata.

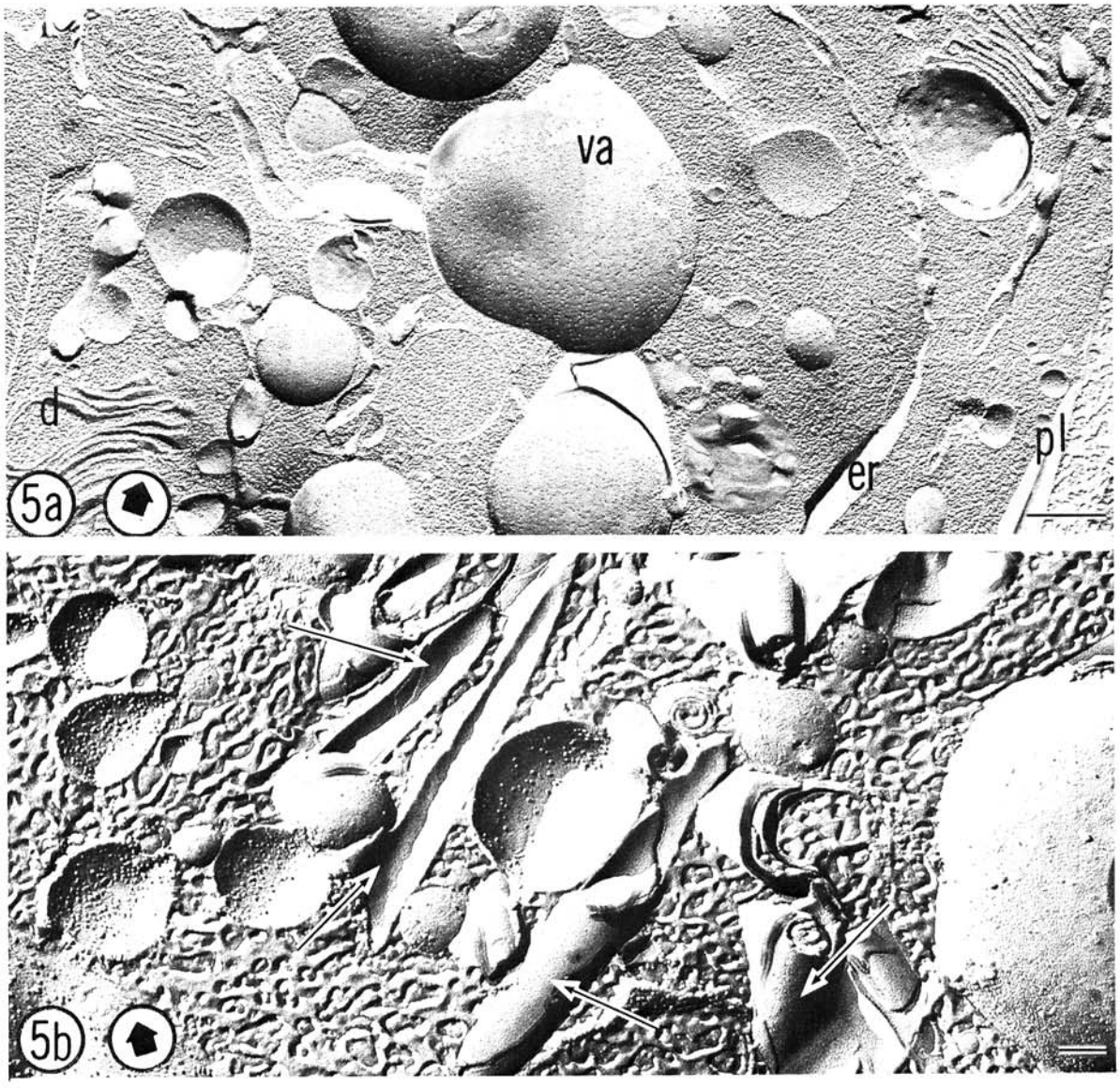

Fig. 5-(a, b). Freeze-etch replicas of tobacco cells. Only the fracture faces are evident. Enclosed arrow indicates shadowing direction. **a)** Noninfected control. Legend: d = dictyosome; va = vacuole; er = endoplasmic reticulum; pl = plasmalemma. × 35,350. **b)** Pinwheel arms in an infected cell (arrows). × 67,200. Scale bars (a) 0.3 μm; (b) 0.1 μm.

The association of pinwheels with plasmodesmata in the meristematic region, where cells are in relatively early stages of infection, indicates that plasmodesmata are the initial sites of pinwheel formation in root cells. Moreover, it is evident from serial sections that many pinwheels which appeared to be free in the cytoplasm were apposed, at their bases, to the cell wall.

Conformation of pinwheels.—It became apparent from examining serial sections used to ascertain pinwheel origin that the shape of these inclusions was not cylindrical, as is generally described. There was a definite tendency for arm length to increase towards the base. Fig. 6 represents four serial sections wherein the length of two arms on opposite sides of the pinwheel were measured and plotted as a function of distance from the cell wall. Similar results were obtained for 13 of 16 (81%) other pinwheels. These data show that the arms do indeed taper toward the apex of the pinwheel. That pinwheels have an overall conical form is also indicated by their tapered appearance when viewed longitudinally in thin-sections (Fig. 3-a) and in freeze-etch preparations (Fig. 5-b).

From these above observations, TEV-induced pinwheels at least early in development are, as a whole, conically shaped, as represented diagrammatically in Fig. 7. The pinwheel is apposed to the cell wall with its hollow central core directly over a plasmodesma, and extending the length of the inclusion. Arms radiating outwards in a spiralled manner are about ten in number, tapered, of various sizes, and occasionally fused.

DISCUSSION.—There is little doubt that a sequence of pinwheel developmental stages occurs in tobacco root tips. Certain cells in the core of the apical meristem are immune to infection and contain no inclusions; whereas, tissues in the root-hair zone are characterized by the presence of large pinwheels. Somewhere in between these two regions, cells become susceptible to infection. Hence this intermediate zone, as a whole, contains pinwheels in all stages of growth. This type of system has been used by others for histological and cytochemical investigations of virus-infected plants (29, 30), but not heretofore as a means of studying ultrastructural changes in viral infection.

The system is not without its faults, however. Small pinwheels were sometimes found in the root hair zone and relatively large inclusions were occasionally seen in the apical meristem. While the former situation might be expected (since presumably pinwheels would be initiated for some time postinfection), the latter is more difficult to rationalize. Some variation, however, might be anticipated in view of the likelihood of quiescent cells in the promeristem (6) and the variation in meristematic activity of cells in the apical meristem (17).

The timing of harvesting roots after inoculation appeared critical. Generally, roots from nonvigorous plants, or plants infected more than 3 wk showed no definitive sequence in pinwheel formation, possibly because the host was in a deteriorating condition and cells in the apical meristem were no longer immune. Finally, and perhaps most important, it is possible that the apparent changes in pinwheels were more a reflection of cellular maturation and differentiation than advancing infection.

Whereas Smith and Schlegel (29) found that viral concn decreased towards the apex of *Vicia faba* roots infected with clover yellow mosaic virus, electron microscopy and infectivity data indicate that the reverse was true in TEV-infected roots. This might be explained

TABLE 1. Association between transversely sectioned pinwheels and plasmodesmata from an analysis of serial sections of root tips of *Nicotiana tabacum* plants infected with tobacco etch virus

Section series	Number of pinwheels followed in serial sections	Number traceable to plasmodesmata
1	4	3
2	6	6
3	2	2
4	2	2
5	3	3
6	2	1
7	8	6
8	3	3
9	2	1
10	3	2
Totals	35	29

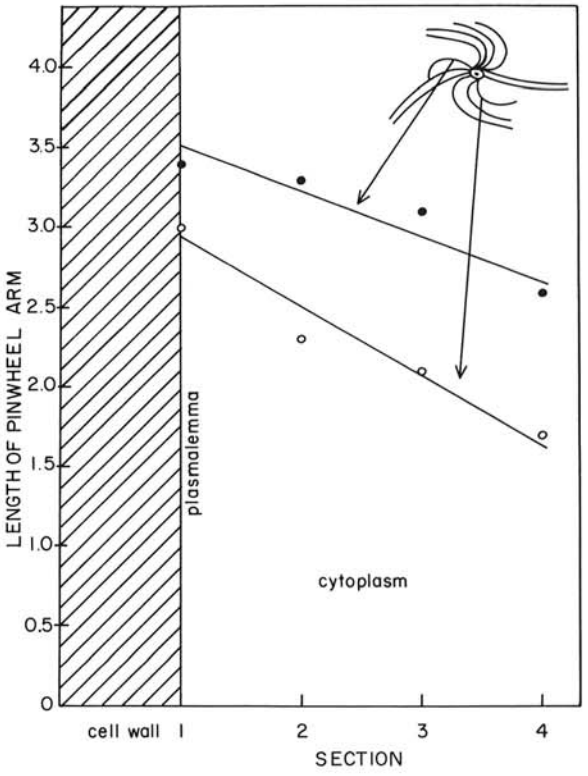

Fig. 6. Lengths of two arms from opposite sides of a pinwheel as a function of distance from the cell wall in four serial sections of tobacco etch virus-infected tobacco root cells. Note that both arms are longest at the plasmalemma and progressively decrease with increasing distance into the cytoplasm. Scale for ordinate: 1 unit = 120 nm.

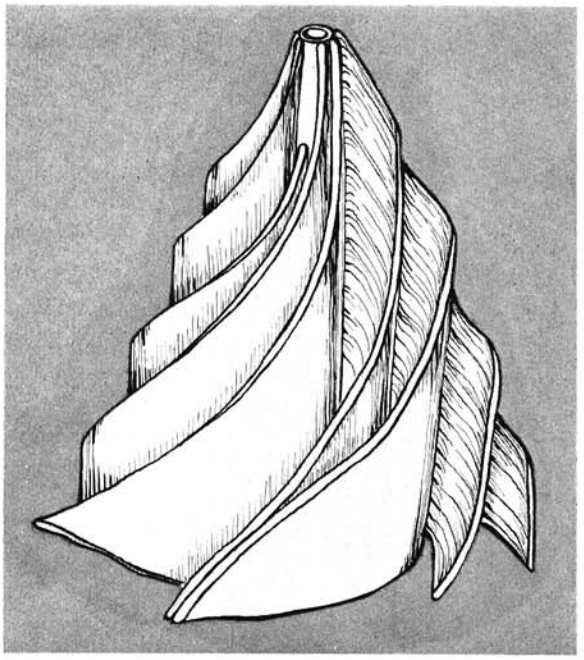

Fig. 7. Model of a pinwheel-type inclusion body consistent with the experimental data for tobacco etch virus-infected tobacco root cells. Note the hollow central core and the spiralled, tapering arms of various sizes, two of which are fused.

on the basis of inhibitors in older parts of the root, or the lower metabolic activity of cells in the root hair zone.

Since pinwheels were present under various fixative conditions, and in freeze-etched tissues (where chemical fixatives were omitted entirely), it is unlikely that they are artifacts of sample preparations. Furthermore, pinwheels induced by a variety of viruses have been examined in a number of hosts, under varying conditions of fixation (see, for example, 14, 32). Hence, they can be considered real structures.

Pinwheels were associated with plasmodesmata, at least in their early stages of formation. Whether they originated there or were transported to these sites after forming elsewhere is not known. However, in cells which had recently become infected, pinwheels were found only abutted to walls, and virtually always aligned precisely over plasmodesmata. The most reasonable interpretation is that, indeed, they were formed there. Lawson and Hearon (19) and Lawson et al. (20) arrived at the same conclusion from a study of russet crack virus in *Ipomea setosa*. Of course it cannot be ruled out that pinwheels may also form elsewhere in the cell. Developmental studies are needed using other types of tobacco tissue to determine whether the formation of TEV pinwheels at plasmodesmata is a general phenomenon, or one peculiar to root cells.

Whether the association between plasmodesmata and pinwheels has any functional significance is a matter for speculation. Although there is obviously an intimate spatial relationship between developing pinwheels and plasmodesmata, we have no evidence to suggest that the central axis of an inclusion derives from an extruded desmotubule. It could be assumed a priori, that pinwheels originate at plasmodesmata because conditions there are most favorable for their formation. Since endoplasmic reticulum (ER) is often associated with plasmodesmata, the ER may be involved in the formation of these large proteinaceous inclusions. An association between ER and pinwheels has been noted frequently (e.g., 2, 14). If pinwheels do form at plasmodesmata, they could play some regulatory role in the intercellular transport of virions and various metabolites. Such a regulatory role would presumably be most effective during the early stages of infection when inclusions attached to plasmodesmata might delay systemic distribution of virions, thereby allowing time for the activation of other host defenses. It is likely that pinwheels, whether attached to cell walls or free in the cytoplasm, would influence cytoplasmic streaming.

Evidence from serial sections points to the conclusion that pinwheel arms are triangular. Therefore, the inclusions as a whole must be conical at least in the early stages of development, and the term "cylindrical" does not correctly describe them.

The sequence of events in pinwheel development is as follows: Pinwheels originate at plasmodesmata where the inclusion core or axis acts as a 'hub' from which a basic complement of 8-10 arms develops more or less simultaneously. The core extends vertically into the cytoplasm in sequence with the arms which taper as they spiral away from the axis. There is a progressive tendency for addition of arms, for arms to fuse, and for the central core to open. Ultimately, massive laminations are formed. At all these stages, but particularly early in development, virus particles can be found intimately associated with pinwheel arms.

Whether pinwheels play some role in the regulation of intercellular transport, as this study suggests, remains to be determined.

LITERATURE CITED

1. AOKI, S., and L. TAKEBE. 1969. Infection of tobacco mesophyll protoplasts by tobacco mosaic virus ribonucleic acid. Virology 39:439-448.
2. ARNOTT, H. J., and K. M. SMITH. 1967. Electron microscopy of virus-infected sunflower leaves. J. Ultrastruct. Res. 19:173-195.
3. BAKER, K. F. 1957. The U.C. system for producing healthy container-grown plants. Manual 23, Calif. Exp. Stn. Ext. Serv., 332 p.
4. BARNETT, O. W., G. A. DE ZOETEN, and G. GAARD. 1971. Bearded iris mosaic virus: transmission, purification, inclusions, and its differentiation from bulbous iris mosaic. Phytopathology 61:926-932.
5. BRANDES, J., and R. BERCKS. 1965. Gross morphology and serology as a basis for classification of elongated plant viruses. Advan. Virus Res. 11:1-24.
6. CLOWES, F. A. L. 1958. Protein synthesis in root meristems. J. Exp. Bot. 9:229-238.
7. CREMER, M. C., D. H. M. VAN SLOGTEREN, and J. A. VAN DER VEKEN. 1961. Intracellular virus inclusions in leaves of 'gray-diseased' narcissus. Proc. Eur. Reg. Conf. on Electron Microscopy, Delft, 1960. Published as de Nederlandse Vereniging voor Electronenmicroscopie, Delft, 1961. 2:974-977.
8. EDWARDSON, J. R. 1966. Cylindrical inclusions in the

cytoplasm of leaf cells infected with tobacco etch virus. Science 153:883-884.
9. EDWARDSON, J. R. 1966. Electron microscopy of cytoplasmic inclusions in cells infected with rod-shaped viruses. Am. J. Bot. 53:359-364.
10. EDWARDSON, J. R., and D. E. PURCIFULL. 1970. Turnip mosaic virus-induced inclusions. Phytopathology 60:85-88.
11. EDWARDSON, J. R., D. E. PURCIFULL, and R. G. CHRISTIE. 1968. Structure of cytoplasmic inclusions in plants infected with rod-shaped viruses. Virology 34:250-263.
12. EDWARDSON, J. R., F. W. ZETTLER, R. G. CHRISTIE, and I. R. EVANS. 1972. A cytological comparison of inclusions as a basis for distinguishing two filamentous legume viruses. J. Gen. Virol. 15:113-118.
13. FINERAN, B. A. 1970. An evaluation of the form of vacuoles in thin sections and freeze-etch replicas of root tips. Protoplasma 70:457-478.
14. HARRISON, B. D., and I. M. ROBERTS. 1971. Pinwheels and crystalline structures induced by Atropa mild mosaic virus, a plant virus with particles 925 nm long. J. Gen. Virol. 10:71-78.
15. HOOPER, G. R., and M. V. WIESE. 1970. Electron microscopy of wheat affected by wheat spindle streak mosaic. Phytopathology 60:1296 (Abstr.).
16. HOOPER, G. R., and M. V. WIESE. 1972. Cytoplasmic inclusions in wheat affected by wheat spindle streak mosaic. Virology 47:664-672.
17. JENSEN, W. A., and L. G. KAVALJIAN. 1958. An analysis of cell morphology and the periodicity of division in the root tip of Allium cepa. Amer. J. Bot. 45:365-372.
18. LANGENBERG, W. G., and H. F. SCHROEDER. 1972. Disruptive influence of osmic acid and unbuffered chromic acid on inclusions of two plant viruses. J. Ultrastruct. Res. 40:513-526.
19. LAWSON, R. H., and S. S. HEARON. 1971. The association of pinwheel inclusions with plasmodesmata. Virology 44:454-456.
20. LAWSON, R. H., S. S. HEARON, and F. F. SMITH. 1971. Development of pinwheel inclusions associated with sweet potato russet crack virus. Virology 46:453-463.
21. MATSUI, C., and A. YAMAGUCHI. 1964. Electron microscopy of host cells infected with tobacco etch virus. I. Fine structures of leaf cells at later stages of infection. Virology 22:40-47.
22. MATSUI, C., and A. YAMAGUCHI. 1964. Electron microscopy of host cells infected with tobacco etch virus. II. Fine structures of leaf cells before and after the appearance of external symptoms. Virology 23:346-353.
23. MOOR, H. 1966. Use of freeze-etching in the study of biological ultrastructure. Int. Rev. Exp. Pathol. 5:179-216.
24. MURANT, A. F., and I. M. ROBERTS. 1971. Cylindrical inclusions in coriander leaf cells infected with parsnip mosaic virus. J. Gen. Virol. 10:65-70.
25. PLUMB, R. T., and D. A. VINCE. 1971. Fixation and electron microscopy of the Rothamsted culture of henbane mosaic virus. J. Gen. Virol. 13:357-359.
26. RUBIO-HUERTOS, M., and F. GARCIA-HIDALGO. 1964. Ultrathin sections of intranuclear and intracytoplasmic inclusions induced by severe etch virus. Virology 24:84-90.
27. RUBIO-HUERTOS, M., and D. LOPEZ-ABELLA. 1966. Ultraestructura de celulas de pimiento infectadas con un virus y su localizaction en las mismas. Microbiol. Espan. 19:77-86.
28. SASS, J. E. 1958. Botanical microtechnique. 3rd. ed., Iowa State Univ. Press, Ames, 228 p.
29. SMITH, S. H., and D. E. SCHLEGEL. 1964. The distribution of clover yellow mosaic virus in Vicia faba root tips. Phytopathology 54:1273-1274.
30. SMITH, S. H., and D. E. SCHLEGEL. 1965. The incorporation of ribonucleic acid precursors in healthy and virus-infected plant cells. Virology 26:180-189.
31. SPURR, A. R. 1969. A low-viscosity epoxy resin embedding medium for electron microscopy. J. Ultrastruct. Res. 26:31-43.
32. WEINTRAUB, M., and H. W. J. RAGETLI. 1970. Distribution of virus-like particles in leaf cells of Dianthus barbatus infected with carnation vein mottle virus. Virology 40:868-881.
33. WILLIAMS, R. C., and F. KALLMAN. 1955. Interpretations of electron micrographs of single and serial sections. J. Biophys, Biochem. Cytol. 1:301-314.